Hydrodynamic Voltammetry at the Liquid/Liquid Interface: The Rotating Diffusion Cell

Brett Kralj and Robert A. W. Dryfe*

Department of Chemistry, University of Manchester Institute of Science & Technology, P.O. Box 88, Manchester M60 1QD, U.K.

Received: February 24, 2002

Hydrodynamic voltammetry is reported at the interface between two immiscible electrolyte solutions (ITIES), using a rotating diffusion cell configuration. The voltammetry arises from laminar flow, induced in the organic and aqueous phases of the ITIES separately. The ITIES has been stabilized by a polyester (PET) track-etched membrane material. The resultant voltammetry is shown to be in accord with the Koutecký-Levich equation for limiting currents at rotating electrodes. The technique is promising for the determination of reaction mechanisms and kinetic parameters for reactions involving immiscible liquid phases.

Introduction

Chemical processes involving immiscible liquid phases are of widespread significance industrially[1,2] and biologically.[3] Understanding of processes at these interfaces is complicated by the dynamic nature of the liquid−liquid interface and difficulties associated with its structural characterization. The electrochemical study of ion transfer at the interface between two immiscible electrolyte solutions (ITIES) has allowed relevant thermodynamic and transport parameters to be determined,[4] although many of the processes measured were limited by diffusion, due to the slow mass-transport rates employed experimentally. A fundamental issue, which remains to be clarified experimentally, is the existence—or otherwise—of an activation barrier to the interfacial transfer of ionic solutes.[5,6] By analogy with interfacial charge transfer at the electrode/electrolyte interface, mass-transport to/from the interface may be enhanced through the introduction of micron,[7,8] or submicron scale interfaces.[9,10] Scanning electrochemical microscopy (SECM) has also been used to probe the liquid/liquid interface.[11,12]

An alternative approach to mass-transport enhancement is through the imposition of convective flow.[13] Liquid−liquid analogues of the dropping mercury electrode have been developed with currents being measured directly by polarization of the ITIES,[14,15] or indirectly by applying an SECM-type approach to the expanding electrolyte droplet.[16] Other hydrodynamic liquid−liquid cells based on the wall-jet electrode configuration[17] and flow-injection have also been reported.[18,19] The latter class of experiment is complicated by the presence of the membrane employed to stabilize the ITIES against flow. Organic gels have been used as alternative routes to stabilize the ITIES in flow experiments,[20] although the relationship between processes at the liquid−liquid interface and the solution−gel interface is unclear. Flow of the aqueous phase in a channel configuration over an organic gel has been reported.[21]

An alternative approach to the study of liquid−liquid extraction processes is the rotating diffusion cell, introduced by Albery and co-workers in the 1970's. [22,23] Modified versions of this device, central to the work reported here, are depicted in Figures 1 and 2. Albery's device consisted of two solutions separated by a supported liquid membrane. Rotating-disk hydrodynamics were imposed on the outer solution by rotation of the tube containing the inner solution. Albery assumed a similar laminar flow profile was imposed upon the inner solution by the presence of the baffle in the inner phase: ex situ analysis of the extent of extraction appeared to support this assumption.[23] One drawback of this technique was its initial reliance on ex situ detection methods, although a later version included electrochemical detection.[24] No external polarization of the liquid−liquid interface was employed in Albery's experiments: recent rotating-diffusion work by Kontturi et al has investigated the transfer of ionic solutes across supported bilayers under polarized (i.e., potentiostatically controlled)

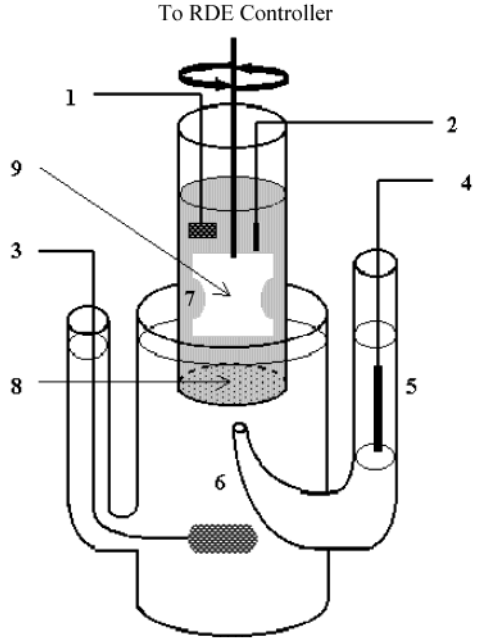

Figure 1. Diagram of the rotating baffle cell used to induce convection on the aqueous side of a PET-supported liquid/liquid interface. **1** is the aqueous phase counter electrode, **2** the aqueous phase reference electrode, **3** and **4** are the organic phase counter and reference electrodes, **5** is the reference solution for the organic phase, **6** is the organic phase, **7** is the aqueous phase, **8** is the PET membrane, and **9** is the rotating baffle.

* Author to whom correspondence should be addressed. Fax: +44 (0)161 200 4559. E-mail: robert.dryfe@umist.ac.uk.

10.1021/jp025683e CCC: $22.00
Published on Web 06/07/2002

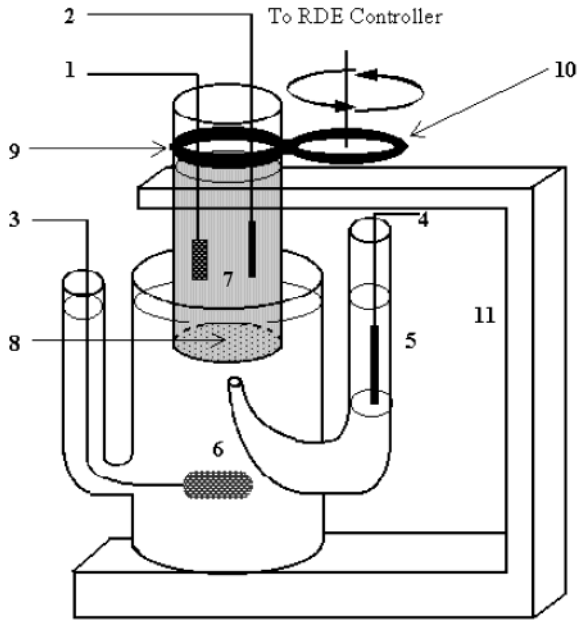

Figure 2. Diagram of the rotating disk cell used to induce convection on the organic side of a PET-supported liquid/liquid interface. **1** is the aqueous phase counter electrode, **2** the aqueous phase reference electrode, **3** and **4** are the organic phase counter and reference electrodes, **5** is the reference solution for the organic phase, **6** is the organic phase, **7** is the aqueous phase, **8** is the PET membrane, **9** is a cog fitted around the glass tube, **10** is a cog which is connected to a RDE controller and interlocked with the cog on the glass tube, and **11** is a Perspex stand.

conditions.[25,26] Both steady-state and transient experiments were reported, although the kinetic parameters derived have been at variance with reports at the ITIES,[9] possibly due to the complexity of the bilayer structure and the consequent uncertainties with regard to the interfacial potential distribution. The rotating diffusion cell has recently been employed in conjunction with radio-labeling to determine the kinetics of the extraction of acetic acid across the water/organic interface.[27]

In a preliminary communication, we have reported how commercially available PET membrane materials may be used to alter the voltammetric response of the ITIES.[28] Specifically, ion transfer through the pores of track-etched PET membranes was reported. Such track-etched membranes are particularly advantageous for the modification of electrified interfaces: among their useful properties are chemical stability, low tortuousity, availability with submicron pore diameters, a small size distribution, and the one-dimensional nature of the pore structure. Moreover, the PET membranes do not swell on contact with the organic solvents employed, in contrast to other materials used to modify the ITIES.[29] This report extends the work describing the effect of such materials on charge-transfer processes at metallic electrodes,[30] and the ITIES under stationary (diffusion-controlled) conditions[31] to a rotating diffusion cell configuration. Specifically, voltammetry associated with the transfer of the tetraethylammonium (TEA^+) cation across the water/1,2-dichloroethane (DCE) interface is discussed. The experimental conditions involve the separate imposition of convective flow on the organic phase and aqueous phases.

Theory

Previous work has shown that modification of the ITIES with PET membranes generates an ensemble of micron-scale ITIES, with the water/DCE interface located within the pores of the ensemble.[28,31] The resultant voltammetric response has been characterized under stationary conditions and shown, in the case of membrane **M1** (see Experimental Section), to result from the overlap of the individual radial diffusion fields at each pore. The resultant linear diffusive response leads to a peak current (I_p) given by eq 1:[32]

$$I_p = 0.4463\left(\frac{z^3F^3}{RT}\right)^{1/2} AD^{1/2}C_b\nu^{1/2} \quad (1)$$

where z is the charge of the transferring ion, υ is the scan rate, F is Faraday's constant, C_b is the bulk concentration of transferring ion, D is the diffusion coefficient of the ion, A is the area of the ITIES (vide infra) while R and T have their usual meanings. Such an overlap is a function of the time scale of the voltammogram and the fraction of surface that is "active" $(1 - \theta)$, i.e., the total pore area compared to the geometric surface area in the case of the PET membranes.[33] The relevant physical parameters for membranes **M1** and **M2**, including the pore density (ρ), are given in Table 1. In the case of a complete overlap of diffusion fields, A is the surface area of the entire membrane exposed to the ITIES.

TABLE 1: Physical Properties of the PET Membranes Used in This Study

membrane	pore radius (r) $\pm$ 0−20%/μm	pore density (ρ) $\pm$ 15%/pores cm^{-2}	nominal thickness (L)/μm	fractional coverage (θ)
M1	5×10^{-2}	4×10^8	6	0.969
M2	0.5	2×10^7	11	0.842

To our knowledge, no theory has been presented to describe the effect of rotation on microelectrode ensembles, although such experiments have been reported for composite (solid) electrodes.[34] Analysis of these experiments was complicated by uncertainties in the geometry of the composite electrode surfaces, leading to uncertainties in θ. Nevertheless, the authors were able to distinguish between radial diffusion and linear diffusion regimes through the dependence of the measured current on rotation speed. Approximate analytical expressions have been presented for voltammetry at electrode arrays/ensembles in the presence of convection, although the earliest work assumed the concentration profile over the electrode was uniform whereas subsequent work did not consider the radial diffusive flux, thus these reports are of limited applicability.[35,36] Levart has used finite-difference methods to compute the currents flowing at rotating-disk electrode arrays, including both radial diffusive and convective terms; however, the simulations were performed for restricted θ values, with an unrealistically low number of array elements.[37]

Given that a linear diffusion field has been established in the absence of external convection for membrane **M1**,[30,31] rotation of the ITIES may be expected to give rise to a steady-state convective-diffusive flux with a limiting current, I_{lim}, described by the Levich equation for a "macro-sized" rotating disk:[38]

$$I_{lim} = 0.62nFAD^{2/3}\mu^{-1/6}C_b\omega^{1/2} \quad (2)$$

where ω is the rotation speed and μ is the kinematic viscosity of the solution. The general trend observed with the composite electrodes was that a linear dependence of I_{lim} on the square root of rotation speed was seen for lower θ values; however, an increase in θ led to a deviation from Levich behavior.

The other limiting case of the microelectrode ensemble is where no overlap of the individual diffusion fields occurs: in this case, a steady-state current, fed by radial diffusion rather than flow, would be established:[31]

$$I_{\mathrm{lim}} = \rho A(4zFDC_{\mathrm{b}}r) \tag{3}$$

where r is the radius of the elements of the array (in this case, the radius of the membrane pores). Equation 3 is a limiting case, which assumes that the ITIES is coplanar with respect to the surface of the membrane. Given the dynamic nature of the ITIES, the interface may in fact be recessed with respect to the membrane to differing degrees.[31,39] The influence of factors other than convective-diffusion on rotating-disk voltammetry, such as charge-transfer kinetics or the presence of a film on the electrode surface, can be assessed through a Koutecký-Levich plot:[40]

$$\frac{1}{I_{\mathrm{lim}}} = \kappa + \frac{\nu^{1/6}}{0.62nFAD^{2/3}C_{\mathrm{b}}\omega^{1/2}} \tag{4}$$

where the intercept κ is defined as

$$\kappa = \frac{1}{I_{\mathrm{lim}}^{\infty}} \tag{5}$$

and $I_{\mathrm{lim}}^{\infty}$ is the limiting current extrapolated to infinitely high rotation speeds, obtained from the vertical intercept of eq 4. Previous reports have described the rotation of single microelectrodes: no complete theoretical treatment is available, but the general observation was of a linear relationship between I_{lim}^{-1} and $\omega^{-1/2}$ for sufficiently high ω, where convection swamped the flux due to radial diffusion.[41−43] These experiments were, however, complicated by difficulties in ensuring that the microdisk electrode was positioned exactly on the axis of rotation.[42,43]

Experimental

Voltammetric experiments were performed with an Autolab PGSTAT 20 potentiostat supplied by Eco-Chemie (Utrecht, Netherlands) which was operated in four-electrode mode. Ohmic compensation was applied via the positive feedback method. All potentials are quoted with respect to Ag/AgCl since the aqueous and organic electrodes reference electrodes were Ag/AgCl wires (CH Instruments, Cordova, TN). The counter electrodes were constructed in-house by spot welding a 1 cm^2 area of platinum gauze (Advent, Eynsham, Oxon, U.K.) to a length of platinum wire (Advent). The PET membranes, obtained as disks of 25 mm diameter, were trimmed and attached to a 7 mm i.d. glass tube with silicone sealant (RS Components, Corby, U.K.). The area of the membrane exposed at the ITIES was varied by treatment of the affixed membrane with further silicone rubber. The PET track-etched membranes were obtained with either 0.1 μm (membrane **M1**) or 1.0 μm (membrane **M2**) diameter pores from Poretics products (Osmonics Corp., Livermore, CA). The manufacturing tolerance for the PET membranes is 0−20% of the stated pore size for 96% of the pores. Table 1 lists the specification for the two types of membrane used.

Two distinct types of cell were employed in this study, namely the rotating baffle cell and the liquid/liquid rotating disk cell, these are discussed in turn next.

The Rotating Baffle. Figure 1 illustrates the experimental setup used to induce convection on the aqueous side of the ITIES. A Teflon baffle is connected directly to a RDE motor controller (EG&G PARC, Princeton, NJ, model 616) enabling it to be rotated at a constant frequency, which in turn generates laminar flow on the aqueous side of the ITIES. The design of the baffle was based on the work of Albery et al.,[22,23] who cut two slots out of the side of a paddle to ensure a re-circulating flow of material in the vessel. The presence of the baffle in the glass tube prevents the use of a Luggin capillary in the aqueous phase; hence, the reference electrode and counter electrode were positioned above the paddle to prevent them from interfering with the rotational motion of the baffle.

The Liquid/Liquid Rotating Disk Electrode. The experimental setup illustrated in Figure 2 shows the liquid/liquid rotating disk electrode used in this study. The glass tube was sealed at one end with the PET membrane and fitted centrally inside a Teflon cog. This cog is interlocked with a second cog, which is directly attached to the RDE controller. Since the two cogs are identical, the rotational frequency of the RDE controller is reproduced by the glass tube, resulting in a hydrodynamic flow analogous to that induced by a RDE on the organic side of the ITIES.

Chemicals. The aqueous phase comprised of 0.1 mol dm^{-3} lithium chloride (Aldrich, Gillingham, U.K.) which was dissolved in water purified using a Milli-Q purification system (Millipore, Watford, U.K.). In the rotating baffle experiments tetraethylammonium chloride (Aldrich) was added to the aqueous phase to give a 1×10^{-3} mol dm^{-3} solution of this salt. The organic phase consisted of 0.02 mol dm^{-3} solution of bis(triphenylphosphoranylidene) ammonium tetraphenylborate in DCE (Lancaster 99%). This electrolyte was prepared by metathesis of bis(triphenylphosphoranylidene) ammonium chloride (Aldrich 97%) and sodium tetraphenylborate (Lancaster, U.K., purity 99%).[44] In the liquid/liquid rotating disk experiments, 1×10^{-3} mol dm^{-3} of tetraethylammonium tetraphenylborate, prepared by metathesis of tetraethylammonium chloride (Aldrich) and sodium tetraphenylborate (Lancaster), were present in the organic phase. The reference electrode for the organic phase was formed by placing an Ag/AgCl reference electrode in an aqueous solution of 1×10^{-3} mol dm^{-3} bis(triphenylphosphoranylidene) ammonium chloride and 0.02 mol dm^{-3} lithium chloride. The cell arrangement for the rotating baffle experiments is designated as cell 1.

Cell 1: $Ag_{(s)}$ | $AgCl_{(s)}$ | BTTPA Cl (1 mM), LiCl (20 mM) $_{(aq)}$ | BTPPA-TPB (20 mM) $_{(1,2-DCE)}$ || TEA Cl (1 mM), LiCl (100 mM) $_{(aq)}$ | $AgCl_{(s)}$ | $Ag_{(s)}$

where the double bar represents the interface to be polarized (the membrane-supported ITIES). The cell arrangement for the liquid/liquid rotating disk electrode is denoted cell 2.

Cell 2: $Ag_{(s)}$ | $AgCl_{(s)}$ | BTTPA Cl (1 mM), LiCl (20 mM) $_{(aq)}$ | BTPPA-TPB (20 mM) $_{(1,2-DCE)}$, TEA TPB (1 mM) || LiCl (100 mM) $_{(aq)}$ | $AgCl_{(s)}$ | $Ag_{(s)}$

Results

A series of cyclic voltammograms recorded using cell 1 at various rotational frequencies, with membranes **M1** and **M2** stabilizing the ITIES, is depicted in Figure 3. The rotating baffle was used to induce convection in the aqueous phase, causing the initial TEA^+ transfer from the aqueous to the organic phase to occur under steady-state conditions. Conversely, the TEA^+

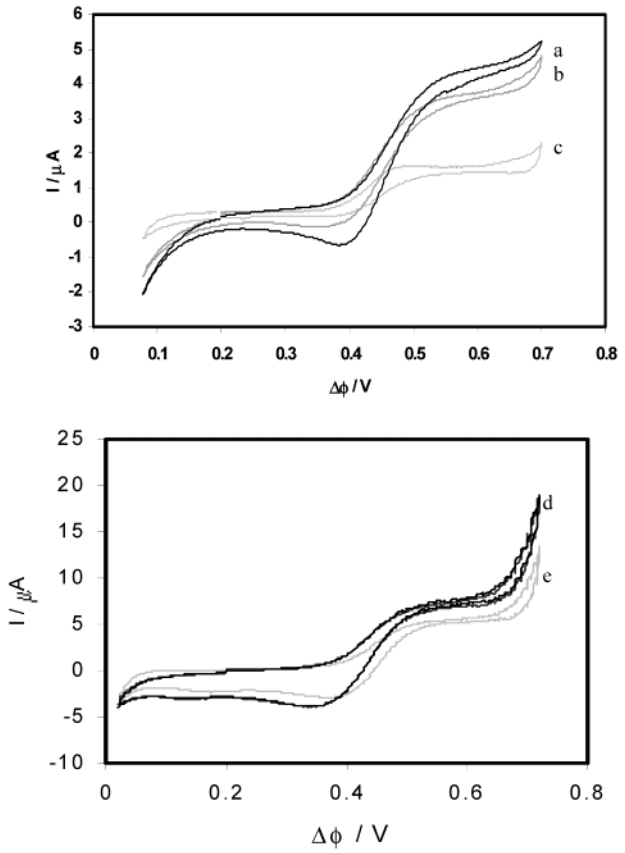

Figure 3. Cyclic voltammetric response obtained using the rotating baffle setup over a range of rotation frequencies (a) 52 rad s^{-1}, (b) 41 rad s^{-1}, (c) 10 rad s^{-1}, (d) 94 rad s^{-1} (e) 41 rad s^{-1} at a scan rate of 5 mV s^{-1} with $C_b = 1 \times 10^{-3}$ mol dm^{-3} for (A) **M1** and (B) **M2**.

returning to the aqueous phase is transported to the ITIES solely by diffusion. This difference in mass transport about the ITIES accounts for the asymmetry observed in the voltammetry for both membrane types and is analogous to the response observed for ion transfer across an ITIES supported within a micropipet.[7,9] For the rotating diffusion experiment, the voltammetry associated with the forward scan (here corresponding to the transfer of TEA^+ from water to DCE) is sigmoidal in shape reflecting the convective-diffusive mode of mass transport, whereas the current functions arising from the reverse scan are peak-shaped, reflecting a diffusion-only mass transport regime. The inference that the steady-state current is a result of the induced convection, rather than a consequence of the radial diffusion to the membrane pores, is based on the results presented in the previous study where membranes **M1** and **M2** were in contact with static immiscible liquid phases.[31] In the static cases, individual diffusion fields associated with each pore were found to overlap with one another creating a single macroscopic diffusion field. This delivers TEA^+ to the ITIES via a linear diffusion regime, which in the present case is augmented by laminar flow on rotation and accounts for the dependence of I_{lim} on the rotation frequency. Another general feature of the voltammetry is the lack of a peak shape on the return peak at low rotation frequencies. At higher scan rates (above 0.05 V s^{-1}) the peak shape can be resolved, which suggests that at low scan rates the Faradaic current is masked by the charging current.

Figure 4 displays the steady-state voltammograms for membranes **M1** and **M2** in terms of eq 4. At rotation speeds greater than 31 rad s^{-1} the reciprocal of the limiting currents obtained experimentally exhibit a linear dependence on $\omega^{-1/2}$. The

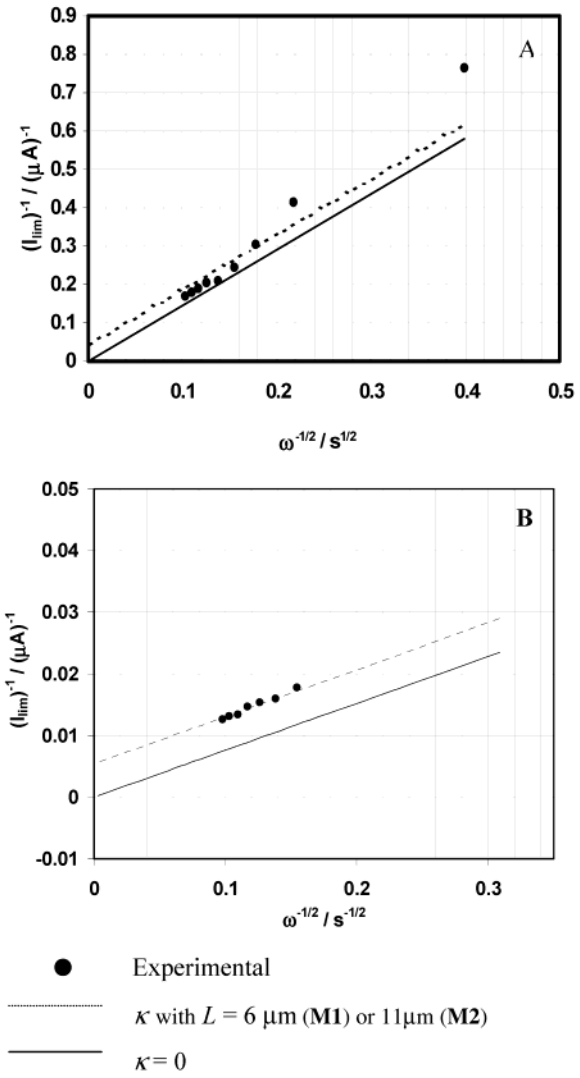

Figure 4. Plot of inverse limiting current, obtained using the rotating baffle for (A) **M1** and (B) **M2**, versus the inverse square root of the rotation speed. Overlaid as a solid line is eq 4 with $\kappa = 0$ and as a dashed line is eq 4 with κ set to the thickness of the membrane (L = 6 μm (**M1**) or 11 μm (**M2**)).

interfacial area was calculated from the gradient of eq 4, using a previously reported value for D,[31] and found to be equal to the measured surface area of the membrane in contact with the ITIES (A). This indicates that the radial diffusion field associated with each member of the ensemble completely overlaps with adjacent members, forming a single macroscopic diffusion field.

Extrapolation of the best-fit straight line in Figure 4 to the intercept (κ) yields information on the system's behavior under conditions of infinite convective mass transport. The nonzero intercept observed can be attributed to three possible factors: (i) interfacial kinetics; (ii) recess of the ITIES within the membranes pores; and (iii) the current becoming dependent on the active surface area, ($A - A\theta$), as opposed to the total geometric area, A. The equations describing factors (i) to (iii), respectively, are[23,31,34]

$$I_{kin}^{\infty} = zFAk^0C_b \tag{6}$$

where k^0 is the standard heterogeneous rate constant;

$$I_{rec}^{\infty} = \frac{zFADC_b\rho\pi r^2}{L} \tag{7}$$

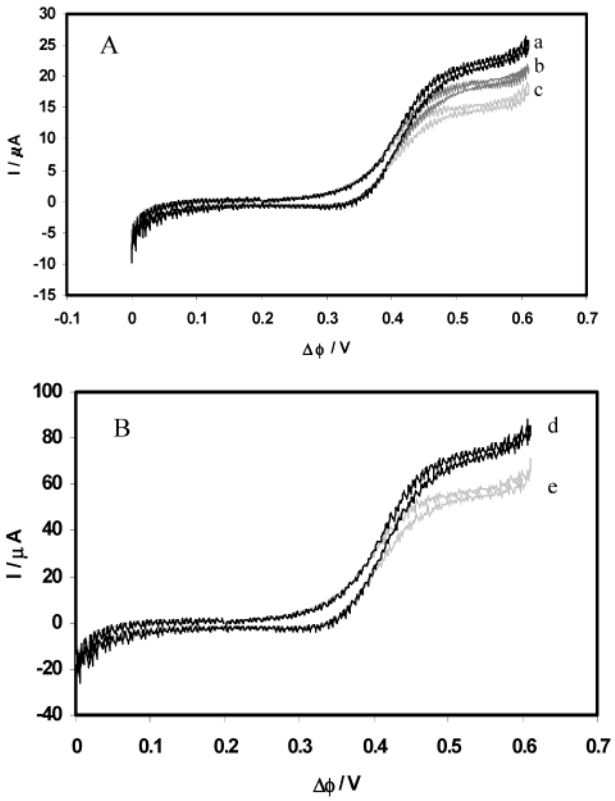

Figure 5. Cyclic voltammetric response obtained using the rotating disk setup over a range of rotation frequencies (a) 52 rad s^{-1}, (b) 31 rad s^{-1}, (c) 10 rad s^{-1}, (d) 94 rad s^{-1} (e) 41 rad s^{-1} at a scan rate of 5 mV s^{-1} with $C_b = 1 \times 10^{-3}$ mol dm^{-3} for (A) **M1** and (B) **M2**.

where L is the distance the ITIES is recessed from the mouth of the pore;

$$I_\theta^\infty = \frac{zFADC_b}{\sum A_N} \tag{8}$$

where ΣA_N is a function determined by the geometry of the membrane,[35] substitution of the parameters associated with membranes **M1** and **M2** into eq 8 gave I_θ^∞ values of 6.2×10^{-4} A and 2.8×10^{-4} A, respectively. From eq 5, the resultant κ values are lower than those determined experimentally, particularly for **M2**, indicating that factors other than surface coverage restrict the mass transport at the high rotation speed limit. It is likely that the observed experimental κ values result from a combination of factors (i) to (iii), hence it is difficult to use the intercept to extract any definitive information on the position of the interface or on interfacial kinetics.

Cyclic voltammograms obtained from cell 2 at various rotational frequencies are depicted in Figure 5. Once more, membranes **M1** and **M2** are used to stabilize the ITIES. The rotating disk in this case induced convection in the organic phase, causing the initial TEA^+ transfer to the aqueous phase to occur under steady-state conditions. The positive currents (in this case, representing transfer of TEA^+ from DCE to water) are sigmoidal in shape, reflecting the convective-diffusive mode of mass transport, with limiting currents that are seen (Figure 6) to increase with rotation speed. Note that the currents on the reverse scan of the voltammogram (aqueous to organic transfer) are also sigmoidal in shape, and retrace those of the forward scan, with little hysteresis. The voltammetry indicates that a symmetrical mass transport regime exists on either side of the ITIES and is thus analogous to the response observed for ion

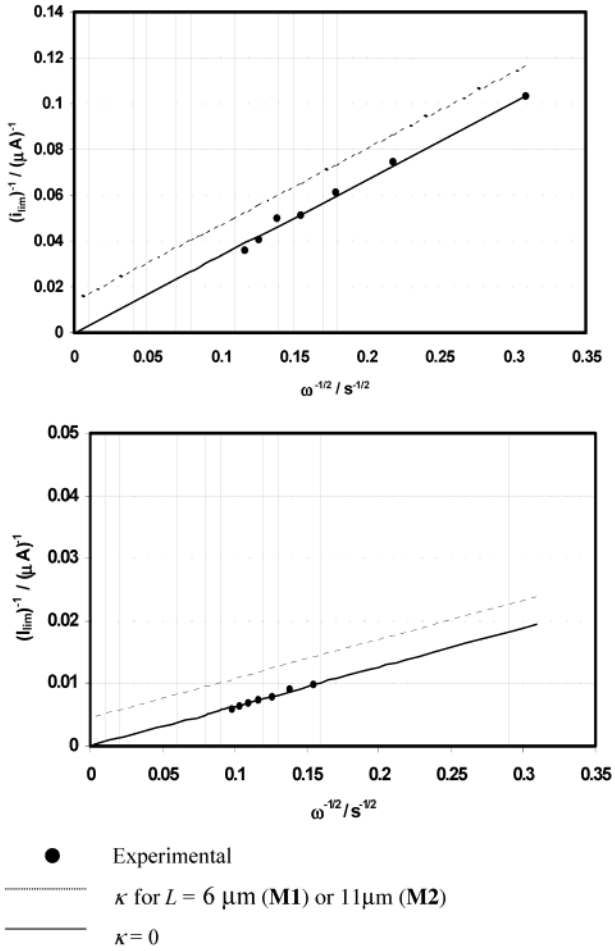

Figure 6. Plot of inverse limiting current, obtained using the rotating disk for (A) **M1** and (B) **M2**, versus the inverse square root of the rotation speed. Overlaid as a solid line is eq 4 with $\kappa = 0$ and as a dashed line is eq 4 with κ set to the thickness of the membrane (L = 6 μm (**M1**) or 11 μm (**M2**)).

transfer across an ITIES supported within a micro-hole.[8,39] The steady-state currents of the reverse scan suggest that a similar hydrodynamic regime is established within the tube, i.e., on the aqueous side of the ITIES. Therefore, rotation of the glass tube supporting the aqueous phase enhances the rate of mass transport to the ITIES from the aqueous phase via convective motion induced in that solution.

Figure 6 plots the steady-state currents for membranes **M1** and **M2** alongside those determined from eq 4 for $\kappa = 0$ and κ calculated for $L = 6$ μm or 11 μm, for **M1** and **M2**, respectively. The reciprocal limiting currents show a linear dependence on $\omega^{-1/2}$. The interfacial area, calculated from eq 4, was found to be equal to the measured surface area of the membrane in contact with the ITIES (A). To this end the diffusion field present in cell 2 is identical to that observed with cell 1 where the radial diffusion field associated with each member of the ensemble completely overlaps with adjacent members.

Extrapolation of the best-fit straight line in Figure 6 to infinite rotation speeds gives a lower κ value for both **M1** and **M2** (1×10^3 A^{-1}) compared to the rotating baffle. Once again the observed experimental κ values can be attributed to a combination of factors (i) to (iii) above, however, because factors (i) and (iii) are identical to those of the baffle experiments, the discrepancy may be attributed to factor (ii), i.e. variation in the interfacial position. The near zero intercept for both **M1** and **M2** implies that the organic phase is only slightly recessed

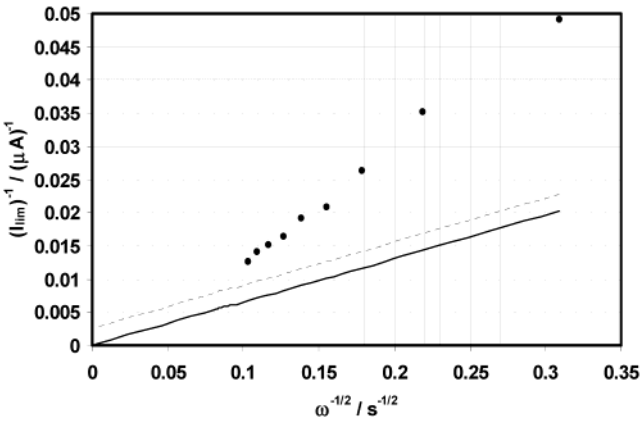

Figure 7. Plot of $1/I_{lim}$ against $\omega^{-1/2}$ for the experimental limiting currents obtained with the rotating baffle and **M1** when the interfacial diameter is comparable to the paddle diameter. Again the solid line was determined from eq 4 with $\kappa = 0$ and the dashed line corresponds to eq 4 with κ set to the thickness of the membrane ($L = 6$ μm).

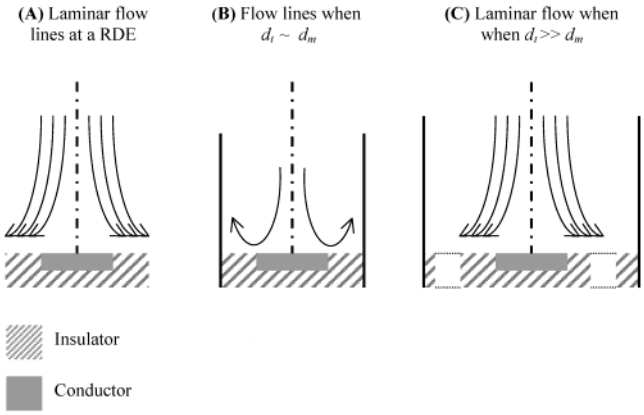

Figure 8. Flow lines at **(A)** a RDE, **(B)** rotating baffle when $d_t \sim d_m$, and **(C)** rotating baffle when $d_t \gg d_m$.

within the pore in this case, i.e., the aqueous phase almost completely fills the pores for cell 2.

In both cell configurations, the diameter of the exposed section of the membrane (d_m) was small compared to the diameter of the paddle: for example in cell 1, d_m was 0.09 cm for the exposed membrane, compared to 0.65 cm for the paddle. This arrangement gave reproducible voltammetry that was consistent with eq 4. By contrast when d_m was increased, for example to 0.3 cm for the data presented in Figure 7, the limiting current response was in poor agreement with eq 4. The poor agreement between experiment and theory with a larger d_m is consistent with the observations made by Albery et al with the nonpolarized rotating diffusion cell.[23] The discrepancy is attributed to the walls of the glass tube perturbing the laminar flow pattern across the membrane. The assumption of laminar flow, as imposed by the rotating disk, is only valid where the dimensions of the cell can be treated as infinite with respect to the dimensions of the active interface (d_m in this case).[45] This is illustrated in Figure 8, where the flow lines to a RDE are compared to the flow induced by the baffle when the diameter of the tube (d_t) is comparable to, or greater than, the diameter of the active membrane (d_m). Thus, an important prerequisite when using a rotating baffle cell is that the diameter of the tube containing the baffle is large with respect to the conducting interface.

Note the position of the ITIES was found in the previous study of stationary solutions to vary over time.[31] This type of behavior may be related to the phenomenon of contact angle hysteresis that has been observed with similar systems, in essence this allows the ITIES to be stable over a range of interfacial positions within the pore.[46] Accordingly, "the history" of the cell becomes relevant in determining where the ITIES is situated: the manner in which the membrane is contacted with the liquid phases and any prior electrification of the cell, e.g., for purposes of Ohmic compensation, may have a bearing on the actual interfacial position. Determining a precise value for L by extrapolation is also complicated by the nonlinear dependence of I_{lim}^{-1} on $\omega^{-1/2}$ at very low rotation speeds, where a steady state is not attained.[34] This deviation from the steady-state response accounts for the points observed for the highest reciprocal I_{lim} values in cells 1 and 2.

TABLE 2: The Mean Apparent Rate Constants and Transfer Coefficient Values Obtained from the Mirkin-Bard Quartile Method

cell 1	$k^0_{app} \pm 0.05$/ cm s^{-1}	α	cell 2	$k^0_{app} \pm 0.05$/ cm s^{-1}	α
M1	0.026	0.55	M1	0.032	0.45
M2	0.033	0.75	M2	0.037	0.70

Given the difficulties described in extracting kinetic information by extrapolation, an alternative method based on the voltammetric wave-shape was employed to evaluate the kinetics of the ion transfer process. The rate of TEA^+ transfer across the ITIES was extracted from the sigmoidal half-cycle of the cyclic voltammogram using the wave-shape method developed by Mirkin and Bard.[47] Table 2 lists the mean apparent rate constants (k^0_{app}) and transfer coefficient (α) values obtained from a series of voltammograms recorded at different rotation speeds using the Mirkin-Bard method, which depends on measurement of the separation between the quartile potentials (where one-quarter and three-quarters of the limiting current flow). Comparison of the theoretical function for a Nernstian sigmoidal voltammogram given by eq 9:[40]

$$I = I_{lim}\left(\frac{1 + e^{\xi}}{e^{\xi}}\right) \tag{9}$$

where:

$$\xi = \frac{zF(\Delta\Phi - \Delta\Phi^0)}{RT} \tag{10}$$

where $\Delta\phi^0$ is the standard potential of transfer, with a voltammogram obtained from cell 2, shows the experimental voltammograms obtained in this study are only slightly displaced from a reversible state, Figure 9. This indicates that the Mirkin-Bard method is being used at the limit of its applicability. The mass transfer coefficient, m^0, can be calculated from eq 11:

$$m^0 = \left(\frac{I_{lim}}{zFAC_b}\right) \tag{11}$$

For the fastest rotation speed ($\omega = 94$ rad s^{-1}) the m^0 value calculated is significantly slower (5.7×10^{-3} cm s^{-1}) than the k^0_{app} values given in Table 2. This discrepancy is due to the effect the modified surface has on the diffusion field. The edge effects present at each micron-sized pore enhance the rate of mass transport beyond that predicted from eq 11. Such effects have been observed for ensembles of microelectrodes in quiescent solution[48] and have been described analytically.[33] The analytical model leads to the conclusion that, under conditions of complete overlap, the measured rate constant k^0_{app} must be

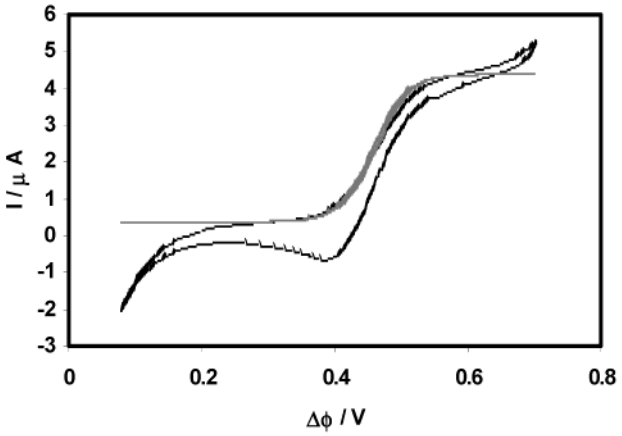

Figure 9. Cyclic voltammogram recorded using cell 1 rotated at a speed of 52 rad s^{-1} with **M1** modifying the ITIES. Overlaid is a theoretical CV determined from eq 9.

TABLE 3: Mean k^0 Values Corrected from Table 2 to Account for the Partially Blocked Surface at the ITIES

cell 1	$k^0 \pm 0.05$/cm s^{-1}	cell 2	$k^0 \pm 0.05$/cm s^{-1}
M1	2.6	M1	3.2
M2	0.82	M2	0.92

adjusted to account for the blocking material, eq 12.

$$k_{app}{}^0 = k^0(1 - \theta_{ens}) \tag{12}$$

where θ_{ens} is the fractional coverage of the blocking film for a random (ensemble) arrangement of microelectrodes, which is given by[49]

$$(1 - \theta_{ens}) = 1 - e^{-\pi\rho r^2} \tag{13}$$

The θ_{ens} values calculated from eq 13 for **M1** and **M2** are 0.01 and 0.04, respectively. If it is assumed the that the above correction holds for the overlapping diffusion field observed under convective-diffusive conditions, inclusion of the factors given in eqs 12 and 13 leads to the k^0 values listed in Table 3.

The k^0 values obtained are self-consistent across the range of rotation speeds and between cell 1 and cell 2, and are also in broad agreement with those reported by Mirkin for TEA^+ transfer.[50] However, there is a considerable error associated with the values obtained, and the rate constants measured using cell 1 are consistently higher than those obtained with cell 2. This uncertainty is attributed to the near-reversibility of the voltammograms obtained (q.v.), which leads to considerable error in the rate constants measured. Consequently, the k^0 values quoted should be considered, more correctly, as lower limits on the value of k^0 for TEA^+ transfer across the water/DCE interface.

Conclusions

A novel hydrodynamic method for the measurement of interfacial charge-transfer processes at the liquid−liquid interface has been presented. The method is based on the rotating diffusion cell and has the advantage of yielding steady-state fluxes that are in agreement with existing models, suggesting that laminar flow profiles are established in both phases. The method has some similarities with the micro-pipet and micro-hole techniques introduced at the liquid−liquid interface; however, the drawbacks associated with these techniques due to uncertainties in interfacial position are minimized through the use of Koutecký-Levich analyses, where extraneous terms appear in the intercept.[40] The high mass-transfer coefficients attainable using the rotating diffusion cell mean this method is a promising route to the measurement of interfacial kinetic parameters. The scope of the kinetic parameters open to measurement from this technique is currently undergoing investigation. Similarly, the extension of this method to other chemical systems, such as ion transfer processes coupled to organic substitution reactions[51] is envisaged.

Acknowledgment. We thank the EPSRC for financial support (Grant reference GR/M73590) and the Leverhulme Trust for the award of a postdoctoral research fellowship to B.K.

References and Notes

(1) Hanna, G. J.; Noble, R. D. *Chem. Rev.* **1985**, *85*, 583.
(2) Atherton, J. H. *Res. Chem. Kinet.* **1994**, *2*, 193.
(3) Tsionsky, M.; Zhou, J.; Amemiya, S.; Fan, F.-R. F.; Bard, A. J.; Dryfe, R. A. W. *Anal. Chem.* **1999**, *71*, 4300.
(4) Girault, H. H. J.; Schiffrin, D. J. In *Electroanalytical Chemistry*; Bard, A. J., Ed.; Marcel Dekker: New York, 1989; Vol. 15, p 1.
(5) Fernandes, P. A.; Cordeiro, M. N. D. S.; Gomes J. A. N. F. *J. Phys. Chem. B* **2000**, *104*, 2278.
(6) Marcus, R. A. *J. Chem. Phys.* **2000**, *113*, 1618.
(7) Taylor, G.; Girault, H. H. *J. Electroanal. Chem.* **1986**, *208*, 179.
(8) Campbell, J. A.; Girault, H. H. *J. Electroanal. Chem.* **1989**, *266*, 465.
(9) Shao, Y.; Mirkin, M. V. *J. Am. Chem. Soc.* **1997**, *119*, 8103.
(10) Liu, B.; Mirkin, M. V. *Electroanalysis* **2000**, *12*, 1433.
(11) Wei, C.; Bard, A. J.; Mirkin, M. V. *J. Phys. Chem.* **1995**, *99*, 16033.
(12) Tsionsky, M.; Bard, A. J.; Mirkin, M. V. *J. Am. Chem. Soc.* **1997**, *119*, 10785.
(13) Compton, R. G.; Fisher, A. C.; Wellington, R. G.; Dobson, P. J.; Leigh, P. A. *J. Phys. Chem.* **1993**, *97*, 10410.
(14) Koryta, J.; Vanýsek, P.; Březina, M. *J. Electroanal. Chem.* **1976**, *67*, 263.
(15) Kihara, S.; Suzuki, M.; Maeda, K.; Ogura, K.; Matsui, M. *J. Electroanal. Chem.* **1986**, *210*, 147.
(16) Slevin, C. J.; Unwin, P. R. *Langmuir* **1997**, *13*, 4799.
(17) Wilke, S.; Franzke, H.; Müller, H. *Anal. Chim. Acta* **1992**, *268*, 285.
(18) Wilke, S. *Anal. Chim. Acta* **1994**, *295*, 165.
(19) Hundhammer, B.; Solomon, T.; Zerihun, T.; Abegaz, M.; Bekele, A.; Graichen, K. *J. Electroanal. Chem.* **1994**, *371*, 1.
(20) Maraček, V.; Jänchenová, H.; Colombini, M. P.; Papoff, P. *J. Electroanal. Chem.* **1987**, *217*, 213.
(21) Liljeroth, P.; Johans, C.; Kontturi, K.; Manzanares, J. A. *J. Electroanal. Chem.* **2000**, *483*, 37.
(22) Albery, W. J.; Couper, A. M.; Hadgraft, J.; Ryan, C. *J. Chem. Soc., Faraday Trans. 1* **1974**, *70*, 1124.
(23) Albery, W. J.; Burke, J. F.; Leffler, E. B.; Hadgraft, J. *J. Chem. Soc., Faraday Trans. 1* **1976**, *72*, 1618.
(24) Albery, W. J.; Choudhury, R. A. *J. Phys. Chem.* **1988**, *92*, 1142.
(25) Manzanares, J. A.; Lahtinen, R.; Quinn, B.; Kontturi, K.; Schiffrin, D. J. *Electrochim. Acta* **1998**, *44*, 59.
(26) Barker, M. H.; Murtomäki, L.; Kontturi, K. *J. Electroanal. Chem.* **2001**, *497*, 61.
(27) Simonin, J. P.; Hendrawan, H. *J. Phys. Chem. B* **2000**, *104*, 7163.
(28) Dryfe, R. A. W.; Kralj, B. *Electrochem. Commun.* **1999**, *1*, 128.
(29) Hundhammer, B.; Dhawan, S. K.; Bekele, A.; Seidlitz, H. J. *J. Electroanal. Chem.* **1987**, *217*, 253.
(30) Kralj, B.; Dryfe, R. A. W. *Phys. Chem. Chem. Phys.* **2001**, *3*, 3156.
(31) Kralj, B.; Dryfe, R. A. W. *Phys. Chem. Chem. Phys.* **2001**, *3*, 5274.
(32) Bard, A. J.; Faulkner, L. R. *Electrochemical Methods*, 2nd ed.; Wiley: New York, 2001; p 231.
(33) Amatore, C.; Savéant, J. M.; Tessier, D. *J. Electroanal. Chem.* **1983**, *147*, 39.
(34) Vitt, J. E.; Johnson, D. C.; Tallmann, D. E. *Anal. Chem.* **1993**, *65*, 231.
(35) Scheller, F.; Müller, S.; Landsberg, R.; Spitzre, H. J. *J. Electroanal. Chem.* **1968**, *19*, 187.
(36) Filinovsky, V. Y. *Electrochim. Acta* **1980**, *25*, 309.
(37) Levart, E. *J. Electroanal. Chem.* **1985**, *187*, 247.
(38) Bard, A. J.; Faulkner, L. R. *Electrochemical Methods*, 2nd ed.; Wiley: New York, 2001; p 339.
(39) Ohde, H.; Uehara, A.; Yoshida, Y.; Maeda, K.; Kihara, S. *J. Electroanal. Chem.* **2001**, *496*, 110.
(40) Bard, A. J.; Faulkner, L. R. *Electrochemical Methods*, 2nd ed.; Wiley: New York, 2001; p 341.
(41) Wang, J. *J. Electroanal. Chem.* **1982**, *140*, 141.

(42) Mallouk, T. E.; Cammarata, V.; Crayston, J. A.; Wrighton, M. S. *J. Phys. Chem.* **1986**, *90*, 2150.
(43) Gao, X.; White, H. S. *Anal. Chem.* **1995**, *67*, 4057.
(44) Shao, Y.; Stewart, A. A.; Girault, H. H. *J. Chem. Soc., Faraday Trans*. **1991**, *87*, 2593.
(45) Levich, V. G. *Physicochemical Hydrodynamics*; Prentice Hall: Englewood Cliffs, NJ, 1962; p 70.
(46) Perwuelz, A.; De Olivera, T. N.; Caze, C. *Colloids Surf. A* **1999**, *147*, 317.
(47) Mirkin, M. V.; Bard, A. J. *Anal. Chem.* **1992**, *64*, 2293.
(48) Cheng, I. F.; Whiteley, L. D.; Martin, C. R. *Anal. Chem.* **1989**, *61*, 762.
(49) Scharifker, B. R. *J. Electroanal. Chem.* **1988**, *240*, 61.
(50) Mirkin, M. V. *Heyrovsky Discussions*; Castle Trest: Czech Republic, June 2001.
(51) Forssten, C.; Kontturi, K.; Murtomäki, L.; Hailes, H. C.; Williams, D. E. *Electrochem. Commun.* **2001**, *3*, 379.